

S. VELUMANI[✉]
J.A. ASCENCIO

Formation of ZnS nanorods by simple evaporation technique

Instituto Mexicano del Petróleo, Eje Central Lázaro Cárdenas, C.P. 07730, D.F. México

Received: 23 July 2003/Accepted: 29 September 2003

Published online: 4 December 2003 • © Springer-Verlag 2003

ABSTRACT Semiconductor nanocrystals and nanorods whose properties are largely determined by the quantum confinement effect are currently being intensively studied by materials scientists, physicists and chemists. Zinc sulphide (ZnS), a II–VI group semiconductor material possessing a direct band gap of 3.66 eV, has recently been extensively investigated due to its multifaceted applications. We report the synthesis of ZnS nanorods by a simple physical vapor deposition method and an in-detail surface analysis for device applications. Our interest in this material mainly lies behind its use as an *n*-window layer for our investigations on different window layers for CdTe- and CIS (Copper Indium diselenide) based solar cells and for photocatalytic production of hydrogen from water using the photocatalysts CdS/ZnS. ZnS films are deposited onto well-cleaned glass substrates at a vacuum of 5×10^{-5} Torr and various parameters are determined. The distance between the substrate and the source was maintained at 0.15 cm. The deposition time was about 20 min at a constant rate of evaporation and the substrates were maintained at room temperature. Structural analysis reveals the cubic nature of the crystallites, which is confirmed from atomic force microscopy (AFM) analysis. The AFM analysis reveals the formation of nanorods due to coalescence, which is substantiated from sectional analysis. A further analysis reveals the preferential growth of the nanorods and the coalescence limited by the energy in the (002) face. The composition was analyzed using an energy-dispersive X-ray method (EDX) and the film was found to possess excess sulfur. The band gap of the vacuum-deposited ZnS film was found to be 3.6 eV.

PACS 61.16.Ch; 79.60.Jv; 61.46.+w; 61.50.Ah

1 Introduction

Recent advances in the synthesis and characterization of nanometer-sized materials continues unabated, and it indicates that more exciting opportunities are lying ahead if the structure can be scaled down to nanometer levels. In the case of semiconductor particles, sizes smaller than the bulk excitonic length become important for observing quantum effects and various technological applications. Zinc sul-

phide (ZnS), a II–VI group semiconductor material, has recently been extensively investigated due to its high potential for various device applications such as *n*-window layers for solar cells, production of hydrogen using the photocatalysts CdS/ZnS, blue-light diodes, electroluminescent displays, photoluminescence, alpha-particle monitoring devices, anti-reflection coatings for infra-red devices, etc. [1, 2]. ZnS is one of the most attractive semiconductors that ensure tunability of the band gap from ultraviolet to visible by employing appropriate dopants. It is of interest as a high-refractive-index material in multilayer optical coatings for various applications. It has a wide band gap of 3.5–3.7 and 3.7–3.8 eV for zinc blende and wurtzite ZnS respectively. It can crystallize in two allotropic forms: a cubic form (c-ZnS) with sphalerite structure and a hexagonal form (h-ZnS) with wurtzite structure. Also, the exciton-binding energy (38 meV) is higher than the room-temperature thermal energy (25 meV), which can provide excitonic emission at room temperature. These features have led us to explore this material for many device applications. For the design and manufacture of multilayers and for various device applications, a good knowledge of surface morphology and structural details of the materials is essential.

Different techniques have been exploited by many scientists for the deposition of ZnS in the form of thin films. ZnS films have been prepared by using molecular beam epitaxy, atomic layer epitaxy, metal-organic chemical vapor deposition, thermal evaporation, radio-frequency (rf) sputtering and hot-wall epitaxy. To the knowledge of the authors, there is no report of nanoparticles or nanorods by any of these techniques except some chemical methods [3, 4] and pressure magnetron sputtering [5].

It is common knowledge that films produced by thermal evaporation in different laboratories (or indeed, in different deposition systems of the same laboratory) have different properties because of the technical difficulties involved in the deposition technique. We report here the formation of nanorods by a simple evaporation technique.

2 Experimental

ZnS (99.99%, Balzers) powder was thermally evaporated by using a vacuum coating unit (Hind Hivac 12A4D) onto cleaned glass substrates under a vacuum of 2×10^{-5} Torr. The distance between the substrate and the

✉ Fax: +52-55/30036429, E-mail: velu@imp.mx

source was maintained at 0.15 m. The rate of evaporation was maintained constant around 2.5 \AA per second throughout the deposition. Initially the substrates were not exposed to the vapor stream by using a shutter, and after obtaining a constant rate of evaporation the shutter was opened and the substrates were exposed for the deposition. The thicknesses of the deposited films were monitored by a built-in quartz-crystal thickness monitor. The thicknesses of the films were verified using a surfometer (Tencor Alpha-Step 100). The structure of the films was analyzed using X-ray diffraction (XRD) (Bruker, Discover D8, using $\text{Cu } K_{\alpha}$ radiation with $\lambda = 0.15418 \text{ nm}$). The composition of the film was analyzed using a Philips scanning electron microscope with attached EDAX (Energy Dispersive Analysis using X-rays) for composition determination. The surface morphology was examined using a Nanoscope4 scanning probe microscope by Digital Instruments, applying the contact mode on the surface. The samples were directly examined without any modifications except to cut them into smaller pieces in order to accommodate them in the sample holder. The optical transmittance spectra are recorded from 400- to 2500-nm wavelength using a Hitachi UV-VIS-NIR spectrophotometer (U-3400) at room temperature with unpolarized radiation on films deposited on glass substrates. The substrate absorption is corrected by introducing an uncoated cleaned glass substrate in the reference beam.

3 Results and discussion

X-ray diffraction is a widely used technique for characterization of thin films because of its nondestructive nature and for completeness of the structural information. In the present study, ZnS films deposited on glass substrates are found to possess a uniform thickness distribution. Figure 1 shows the diffraction pattern and the energy-dispersive X-ray (EDX) spectra of a representative ZnS film on a glass substrate. From the EDX analysis it is found that the films are almost stoichiometric with a small excess of sulfur content ($\text{Zn/S} = 46/54$), while the other identified peaks correspond to the substrate. The most intense diffraction peak for ZnS was observed at 28.75° and can be attributed to either the hexagonal (002) or cubic (111) reflection. The reflections from these two planes cannot be resolved due to their similar d -spacing. There are a number of conflicting reports concerning the crystallographic structure of ZnS films grown using various techniques. Films grown by spray pyrolysis on Si(100) and (111) substrates displayed hexagonal structure above 460°C , while films deposited on Corning glass substrates were found to be cubic above 450°C and hexagonal below 350°C substrate temperature. But atomic force microscopy (AFM) analysis confirms the formation of cubic crystallites deposited by a simple physical vapor deposition technique at room temperature. The cubic formation of the

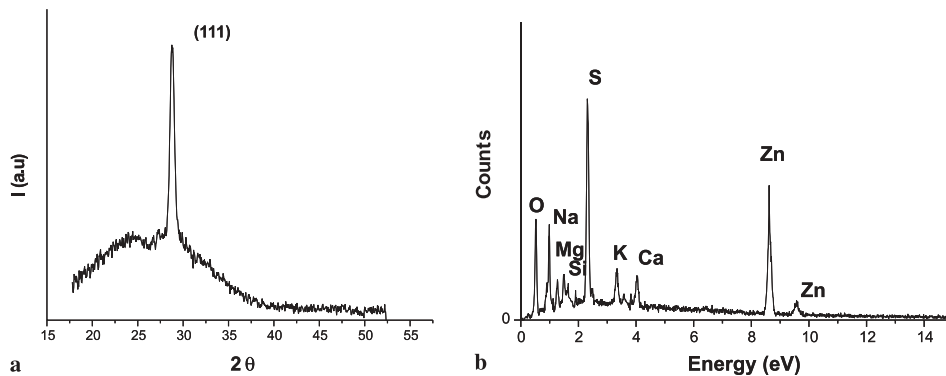


FIGURE 1 a XRD pattern of vacuum-deposited ZnS nanorods showing a preferred orientation along the (111) cubic face, b EDX pattern of the ZnS nanorod showing a slight increase in concentration of S

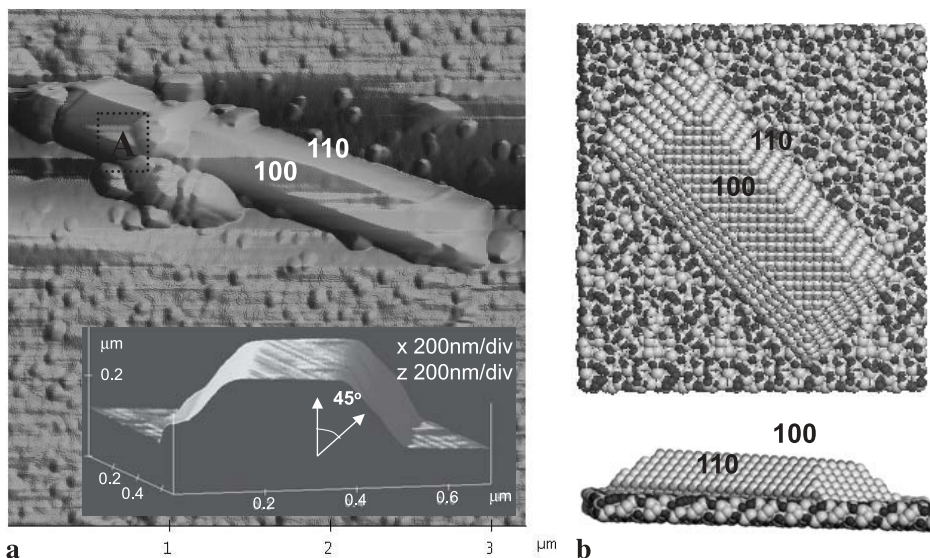


FIGURE 2 a ZnS nanorod observed by AFM; in the marked region (A) particles show a coalescence behavior while the {100} and {110} faces are also marked, whereas in the *inset* a transversal view allows us to identify the angle between the faces as 135° . b From the observed details, a model is shown where the produced faces are identified

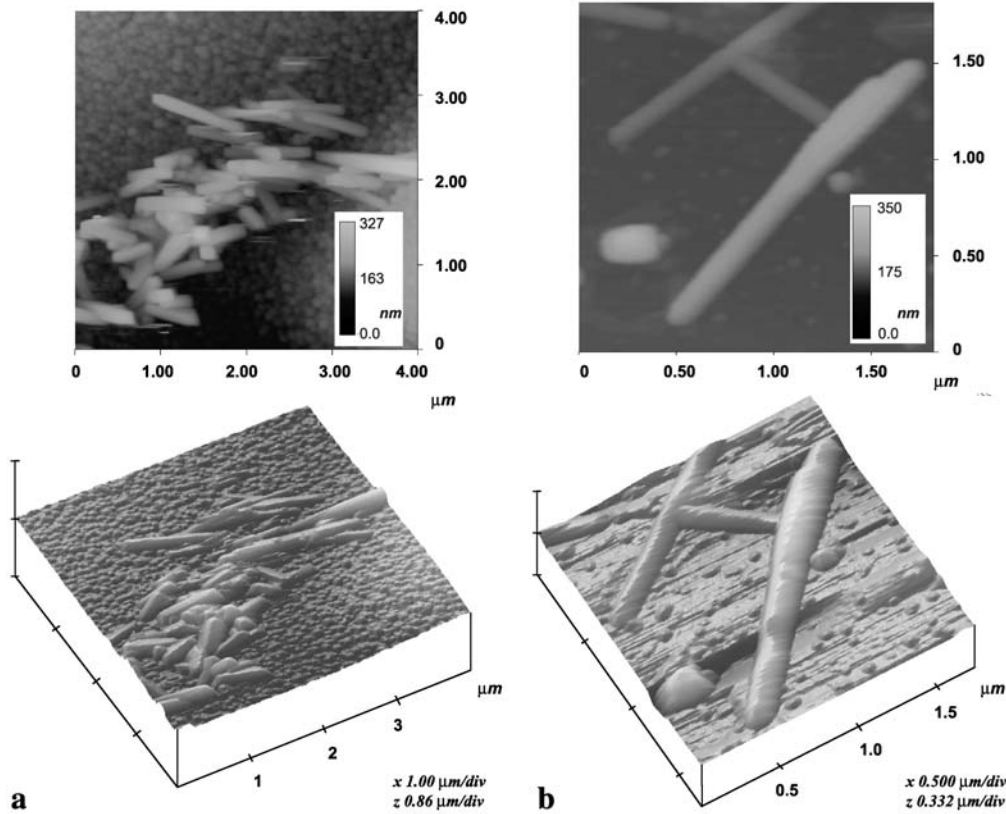


FIGURE 3 AFM micrographs of ZnS nanorods over a glass substrate. **a** A group of rods interacting with varying angles between them where there is no coalescence. **b** Three nanorods, joined with an angle of 90° , which induce coalescence. In both cases the *top image* corresponds to the 2D representation and the *bottom image* shows the 3D reconstruction

crystallites influences the formation of nanorods, which can be associated with the crystalline habits from small particles. The formation of the nanorods under these conditions can be attributed to the coalescence of the small particles during the agglomeration, as clearly depicted in Fig. 2a.

Also, Fig. 2 clearly demonstrates the existence of small particles over the glass substrate, and in the zone marked with A, bigger clusters are coalescing together forming a one-dimensional structure. The new structure is characterized by flat faces and with an apparent vortex forming a symmetric shape.

This faceting behavior can be directly related to an fcc-like crystal habit, for the growing process of nanorods. In fact, considering this growing behavior, it is possible to associate the faces with the classical $\{100\}$ and $\{110\}$ faces for fcc nanorods [6, 7], which are marked in Fig. 2a. These observed details imply a thin fcc-based nanorod, as can be observed in the simulated model shown in Fig. 2b, where the nanorod is reproduced on a glass substrate in two different views for clarity. The model was built considering an fcc crystal, which can also be associated with the morphology by a simple crystalline habit approach, and it presents the exposed $\{100\}$ and $\{110\}$ faces corresponding to the fcc-like nanorod growing behavior.

Besides the direct observation, from the measured angle in the inset of Fig. 2a, we can identify an angle of 135° that is directly related to the angle formed by the $\{100\}$ and $\{110\}$ faces with a simple expression of a vector product as

$$\mathbf{a} \cdot \mathbf{b} = |\mathbf{a}| |\mathbf{b}| \cos \theta \Rightarrow \theta = \arccos \left(\frac{\mathbf{a} \cdot \mathbf{b}}{|\mathbf{a}| |\mathbf{b}|} \right), \quad (1)$$

and that, in our case,

$$(1,0,0) \cdot (1,1,0) = |(1,0,0)| |(1,1,0)| \cos \theta \\ \Rightarrow \theta = \arccos \left(\frac{(1,0,0) \cdot (1,1,0)}{|(1,0,0)| |(1,1,0)|} \right), \quad (2)$$

which implies an angle between them of 45° ; this is also confirmed from the direct measurements.

Particularly, the growing axis can be clearly identified to be perpendicular to the $\{001\}$ face of the fcc nanorod, which matches absolutely with metallic nanorod systems [6, 7]. This axis must establish a preferential direction to grow up the nanorod, and it must also imply a direct limitation for the coalescence of structures at different orientations. In fact, the observation of these ZnS nanorods becomes more common in many other zones on the substrate, where it is possible to identify groups of nanorods with similar dimensions and nearly the same orientation, as can be observed in Fig. 3a where a group of nanorods are identified with angles between them (around 5° to 55°). In the bidimensional representation there could be considered the possibility of coalescence; however in the three-dimensional reconstruction the boundaries are clearly recognized, which must be associated with individual nanorods. In addition, in Fig. 3b three rods match with angles of exactly 90° , which generates a coalescence forming an 'H'. In the 2D image, overlapping could be considered but in the 3D image it is possible to distinguish how the coalescence at 90° is produced. Hence, the preferential axis determines the coalescence when two similar atomically ordered faces are exposed to each other, as in the case of matching of the $\{100\}$ and the $\{001\}$ faces.

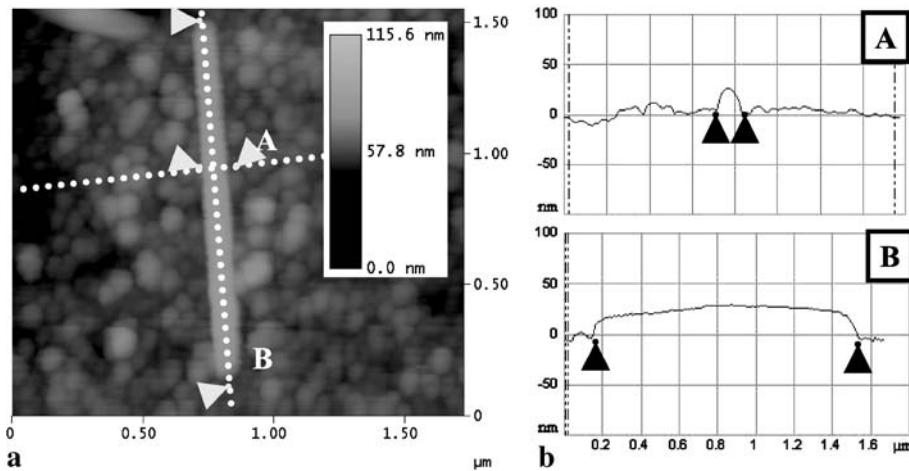


FIGURE 4 ZnS nanorods with a length of 1.415 μm . **a** AFM image and **b** sectional profiles from the lines marked in the image for transversal (A) and longitudinal (B) measurements

The capacity to produce longer nanorods is limited by the energy over the {001} face and the material deposited with the possibility to be coalesced. This implies the possibility to keep growing until very long rods are obtained, as shown in Fig. 4, where a nanorod of 1.415 μm is observed. However, the thickness of these nanorods is not directly related to their length or width. This can be seen from the fact that even when the width of the nanorod is about 138 nm, its thickness is not higher than 30 nm. In the image, it is possible to identify many grains around the nanorods, which are related to the size of the nanorod. The conditions of the formation of the nanorods due to the coalescence of the neighboring particles can be better studied by using a sectional analysis, which allows the determination of the local thickness for a particular section or line. In Fig. 4b the profiles from the lines marked A and B in the image are shown. In these plots, a flat shape can be distinguished for the nanorod and irregular profiles for the neighboring particles in the transverse measurement (A), while for the longitudinal one (B), the longer flat shape of the rod is clearly recognized. The maximum height for the nanorod is observed to be around 30 nm.

From the optical analysis, films showed fairly good transparency above 550 nm. Figure 5 shows the transmittance spectra (the inset showing the band-gap calculation) of a typical ZnS film. Two different plots, $(\alpha h\nu)^{1/2}$ versus $(h\nu)$ and $(\alpha h\nu)^2$ versus $(h\nu)$, were made and it is found that $(\alpha h\nu)^{1/2}$ versus $(h\nu)$ did not lead to straight lines over any part of the optical spectrum, thus supporting the interpretation of a direct band gap rather than an indirect band gap. In the inset of Fig. 5 the $(\alpha h\nu)^2$ versus $(h\nu)$ plot is shown and the straight-line portion of the curve extrapolated to cut the x axis gives the band gap. The band gap of the vacuum-deposited ZnS nanorods in the film form was found to be 3.6 eV. Detailed calculations of the optical constants are made, similar to other semiconductor materials [8]. Also, there is no significant deviation in the band gaps compared to the bulk materials [9].

Hence we conclude that the process of optimizing the deposition conditions to reproduce the ZnS nanorods by a simple evaporation technique is underway. This relatively simple method to produce a one-dimensional ZnS structure opens a new expectation for applications and for nanotechnological developments in the semiconductor field, particularly in its use for solar cells and photonic sensors. Apart from this,

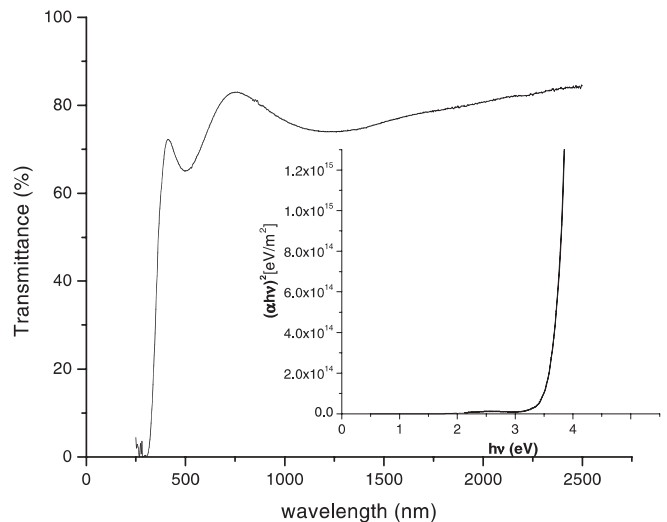


FIGURE 5 Transmittance spectra of a typical ZnS film that includes nanorods; in the *inset* the corresponding $(\alpha h\nu)^2$ versus $(h\nu)$ plot for band-gap calculation is shown

preferential orientation along a particular axis allows a better understanding of the mechanisms to produce controlled junctions in electronic devices using nanorods.

ACKNOWLEDGEMENTS The authors thank Dr. G. Canizal and his students for the AFM analysis of the samples and Dr. P. Del Angel and Dr. M. Espinosa for the XRD and compositional analysis, respectively.

REFERENCES

1. Y.Z. Yoo, T. Chikyow, P. Ahmet, Z.W. Jin, M. Kawasaki, H. Koinuma: *J. Cryst. Growth* **237**, 1594 (2002)
2. A.S. Ethiraj, N. Hebalkar, S.K. Kulkarni, R. Pasricha, J. Urban, C. Dem, M. Schmitt, W. Kiefer, L. Weinhardt, S. Joshi, R. Fink, C. Heske, C. Kumpf, E. Umbach: *J. Chem. Phys.* **118**, 8945 (2003)
3. Z.A. Peng, X. Peng: *J. Am. Chem. Soc.* **123**, 183 (2001)
4. P. Balaz, M. Valko, E. Boldizarova, J. Briancin: *Mater. Lett.* **57**, 188 (2002)
5. S.K. Mandal, S. Chaudhuri, A.K. Pal: *Thin Solid Films* **350**, 209 (1999)
6. M. Jose-Yacamán, J.A. Ascencio, G. Canizal: *Surf. Sci. Lett.* **486**, L449 (2001)
7. P.L. Gai, M.A. Harmer: *Nanoletters* **2**, 771 (2002)
8. S. Velumani, S.K. Narayandass, D. Mangalaraj: *Semicond. Sci. Technol.* **13**, 1016 (1998)
9. S.M.A. Durrani, A.M. Al-Shukri, A. Iob, E.E. Khawaja: *Thin Solid Films* **379**, 199 (2000)